

Received: 23 January 2013 – Accepted: 1 February 2013 – Published: 15 February 2013

Correspondence to: M. D. Gibson (mark.gibson@dal.ca)

Published by Copernicus Publications on behalf of the European Geosciences Union.

ACPD

13, 4491–4533, 2013

Identifying sources driving observed PM_{2.5} variability

M. D. Gibson et al.

Title Page

Abstract

Introduction

Conclusions

References

Tables

Figures



Back

Close

Full Screen / Esc

Printer-friendly Version

Interactive Discussion



Abstract

The source attribution of observed variability of total $PM_{2.5}$ concentrations over Halifax, Nova Scotia was investigated between 11 July–26 August 2011 using measurements of $PM_{2.5}$ mass and $PM_{2.5}$ chemical composition (black carbon, organic matter, anions, cations and 33 elements). This was part of the BORTAS-B (quantifying the impact of Boreal forest fires on Tropospheric oxidants using aircraft and satellites) experiment, which investigated the atmospheric chemistry and transport of seasonal boreal wild fire emissions over eastern Canada in 2011. The US EPA Positive Matrix Factorization (PMF) receptor model was used to determine the average mass (percentage) source contribution over the 45 days, which was estimated to be: Long-Range Transport (LRT) Pollution $1.75 \mu\text{g m}^{-3}$ (47%), LRT Pollution Marine Mixture $1.0 \mu\text{g m}^{-3}$ (27.9%), Vehicles $0.49 \mu\text{g m}^{-3}$ (13.2%), Fugitive Dust $0.23 \mu\text{g m}^{-3}$ (6.3%), Ship Emissions $0.13 \mu\text{g m}^{-3}$ (3.4%) and Refinery $0.081 \mu\text{g m}^{-3}$ (2.2%). The PMF model describes 87% of the observed variability in total $PM_{2.5}$ mass (bias = 0.17 and RSME = $1.5 \mu\text{g m}^{-3}$). The factor identifications are based on chemical markers, and they are supported by air mass back trajectory analysis and local wind direction. Biomass burning plumes, found by other surface and aircraft measurements, were not significant enough to be identified in this analysis. This paper presents the results of the PMF receptor modelling, providing valuable insight into the local and upwind sources impacting surface $PM_{2.5}$ in Halifax during the BORTAS-B mission.

1 Introduction

Numerous studies have shown an association between exposure to ambient fine atmospheric particles, less than or equal to a median aerodynamic diameter of 2.5 microns ($PM_{2.5}$), and acute and chronic health effects (Pope et al., 2002; Dominici et al., 2006). Studies have shown that biomass derived $PM_{2.5}$ is at least as harmful to health as fossil fuel combustion related $PM_{2.5}$ (Allen et al., 2008; Norris et al., 2000). In addition, forest

ACPD

13, 4491–4533, 2013

Identifying sources driving observed $PM_{2.5}$ variability

M. D. Gibson et al.

Title Page

Abstract

Introduction

Conclusions

References

Tables

Figures

◀

▶

◀

▶

Back

Close

Full Screen / Esc

Printer-friendly Version

Interactive Discussion



Identifying sources driving observed PM_{2.5} variability

M. D. Gibson et al.

Title Page

Abstract

Introduction

Conclusions

References

Tables

Figures

⏪

⏩

◀

▶

Back

Close

Full Screen / Esc

Printer-friendly Version

Interactive Discussion



fire derived PM_{2.5} chemical components and associated gases are known to impact climate and local air quality (Parrington et al., 2011; Gambaro et al., 2008). Remote sensing estimates of the 10-yr average number of forest fires each year in North America is 5062, covering an area of 1 323 736 ha, making biomass burning a major source of PM_{2.5} in North America (Palmer et al., 2013).

Because of the importance of understanding the impact of North American boreal forest wildfires on Northern Hemisphere tropospheric chemistry, a multi-national project, led by the University of Edinburgh was conducted out of Halifax, Nova Scotia, Canada during the summer of 2011. The study aim was to quantify the impact of “BOReal forest fires on Tropospheric oxidants over the Atlantic using Aircraft and Satellites”. Central to BORTAS-B was a measurement campaign with the UK Facility for Airborne Atmospheric Measurements (FAAM) BAe146 research aircraft (Parrington et al., 2011; Palmer et al., 2013). In addition, numerous satellite observations of trace pyrogenic gases were made (Tereszchuk et al., 2012).

One component of the BORTAS-B project was to determine the surface impact of boreal forest fire plumes as they were transported across Nova Scotia. This led to the establishment of the Dalhousie University Ground Station (DGS) in Halifax that utilized a variety of instruments to measure size-resolved particulate composition and gas species concentrations both in-situ and through the atmospheric column. The additional BORTAS-B DGS instrumentation not included in this paper are described in Palmer et al. (2013).

Presented here are the results of receptor modelling used to identify the major sources that are responsible for observed variability of total PM_{2.5} in Halifax sampled during the BORTAS-B mission.

2 Measurements

Figure 1 shows the geographical location of the DGS. The DGS is 65 m a.s.l. with the sampling inlets 15 m above ground level on the roof of the Sir James Dunn

**Identifying sources
driving observed
PM_{2.5} variability**

M. D. Gibson et al.

Title Page

Abstract

Introduction

Conclusions

References

Tables

Figures

◀

▶

◀

▶

Back

Close

Full Screen / Esc

Printer-friendly Version

Interactive Discussion



collects PM_{2.5} (fine particles) with the second filter simultaneously collecting PM_{2.5–10} (coarse particles). The Partisol operates by first drawing air through a standard PM₁₀ size selective inlet at a flow rate of 16.7 L min⁻¹ (Gibson et al., 2009). The flow is then split, with 15.0 L min⁻¹ passing through the PM_{2.5} collection filter and 1.67 L min⁻¹ passing through the PM_{2.5–10} collection filter providing a dichotomous sample of fine and coarse PM (Dabek-Zlotorzynska et al., 2011). Only the PM_{2.5} filter was used for source apportionment. The Partisol flow rate was checked weekly with a Dry Cal Defender flow meter. The Partisol stopped sampling if the flow rate deviated by more than ±10% of the set flow. The Partisol flow rate was maintained by an onboard volume flow controller. Because of the volume flow controller the uncertainty of the Partisol flow rate was found to be < 0.5%. Weekly internal and external leak checks were performed on the Partisol as per the manufactures instructions with no failures reported during the study.

Assembly and disassembly of the ChemComb sampler and Partisol filter cassettes was conducted in a Clean-Ceil, high efficiency particle air (HEPA) cleaner hood (Microzone, Corporation, Ottawa, Ontario, Canada, K2S2C7) in the Atmospheric Forensics Research Group (AFRG) laboratory, Department of Process Engineering and Applied Science, Dalhousie University. The Clean-Ceil HEPA hood operated at low flow to provide particle free air while handling filters.

The total PM_{2.5} mass concentration was determined by gravimetric analysis of the Teflon filter sample at Alberta Innovates (Highway 16A and 75th Street, Vegreville, Alberta, Canada, T9C 1T4). The gravimetric analysis was conducted in accordance with USEPA protocol for the determination of ambient PM_{2.5} mass concentration using filter based sampling systems (USEPA, 1998). The Teflon filters used for mass determination were housed in 47 mm contact plates, triple wrapped in airtight Ziplock bags and shipped to, and from, Alberta Innovates in coolers by express airfreight.

After gravimetric determination, the PM_{2.5} Teflon filter samples were shipped in the same fashion to RTI International (3040 Cornwallis Road, Building 7, RTP, NC, USA 27709) for the analysis of 33 elements (Ag, Al, As, Ba, Br, Ca, Cd, Ce, Cl, Co, Cr,

Identifying sources driving observed PM_{2.5} variability

M. D. Gibson et al.

Title Page

Abstract

Introduction

Conclusions

References

Tables

Figures

◀

▶

◀

▶

Back

Close

Full Screen / Esc

Printer-friendly Version

Interactive Discussion



Cs, Cu, Fe, In, K, Mg, Mn, Na, Ni, P, Pb, Rb, S, Sb, Se, Si, Sn, Sr, Ti, V, Zn and Zr) using a Thermo Fisher Scientific Quant’X energy dispersive x-ray fluorescence (ED-XRF) instrument. Due to low PM_{2.5} mass, 14 of the following elements measured by ED-XRF were not detected in any of the samples: Ag, Cd, Ce, Cs, In, P, Pb, Rb, Sb, Se, Sn, Sr, Ti and Zr.

The anions, cations and water soluble metals were extracted from each nylon filter in a clean, 50 mm diameter, screw cap NALGENE extraction bottle.

The nylon filter was then wetted with 100 µL of HPLC grade isopropanol, and extracted with 8 mL Type-1, 18 MΩcm water followed by 30 min sonication. The anion and cation analysis was conducted in the AFRG laboratory using a Thermo Fisher Scientific, Dionex ICS-1000 ion chromatograph (Dionex Canada Ltd, RPO Maple Grove Village, Oakville, Ontario, L6J 7P5). Details of the Dionex instrument configuration and analysis protocol for the anion analysis is reported in Gibson et al. (2013). Cations were analyzed using the Dionex ICS-1000 fitted with an IonPac CS-12 analytical column and guard column, 20 mM methanesulfonic acid eluent with an inject loop of 25 µL. Seven point standard curves were used to quantify both anions and cations. The method used to determine the detection limit of the anions and cations is described in Gibson et al. (2013). Anions and cations not detected by ion chromatography in any of the samples included F⁻, NO₂⁻, Br⁻, HPO₄²⁻ and Mg²⁺. The water soluble metals (P, Cr, Mn, As, Se, Pb and Sr) extracted from the nylon filter were analyzed using a Thermo X-Series II single quadrupole inductively coupled plasma-mass spectrometer (ICP-MS) in the Department of Civil and Resources Engineering at Dalhousie University. A five-point standard curve of the isotope masses ³¹P, ⁵²Cr, ⁵⁵Mn, ⁷⁵As, ⁸²Se, ²⁰⁸Pb and ⁸⁸Sr were used for qualification and quantification. These elements were found to be above the detection limits in all samples.

Black carbon was estimated from continuous 1-min averages of light absorption at 880 nm using a Magee Scientific Corporation, AE42 aethalometer (1916A M. L. King Jr. Way Berkeley CA 94704, USA) (Lawless et al., 2004; Babu and Moorthy, 2002). The mass absorption conversion factor used was 16.6 (Hansen, 2005). The precision of the

AE42 aethalometer was determined by side-by-side comparisons with a second AE42 instrument. The precision of the 1-min averages was found to be 18%. The 1-min data points were integrated to match the 24-h PM_{2.5} filter samples.

An Aerodyne Research, Inc., (Billerica, MA, US, 01821-3976) Aerosol Chemical Speciation Monitor (ACSM) (Ng et al., 2011) was operated by Environment Canada for the purposes of measuring continuous OM, NH₄, SO₄, Cl and NO₃ at a temporal resolution of 30 min. The ACSM, 30-min data points were integrated to match the 24-h PM_{2.5} filter samples. Only the OM from the ACSM was used in the receptor modelling of the PM_{2.5} as the NH₄, SO₄ and Cl from the nylon filter are recognized as the standard protocol for PM_{2.5} speciation used in receptor modelling (Dabek-Zlotorzynska et al., 2011). Filter based samples of OM were not available in this study, hence the use of the ACSM OM. The upper size cutoff (50% transmittance) for the ACSM is close ~ 650 nm and the lower cut is 80–100 nm (Liu et al., 2007). While most of the organic (both primary and secondary) organic aerosol mass is at sizes smaller than 650 nm, it is possible that some of the mass between 650 nm and 2.5 μm was lost (Ng et al., 2011). Mass calibrations were performed before and after the experiment at Environment Canada in Toronto using nearly monodisperse particles of ammonium nitrate. The data completeness for the ACSM during BORTAS-B was 85% (missing data between 2 August and 8 August). Stepwise regression (SR) was used to predict OM during the period of missing data. 21 PM_{2.5} species variables and meteorological variables were used in the SR model. The significant OM predictor variables (*p*-values, coefficient) used in the SR model were K (*p* = 0.001, 10.801), Ni (*p* = 0.007, -204.097), Zn (*p* = 0.0003, 121.884) and SO₄ (*p* < 0.001, 0.531). The SR constant was 0.157 with a model *r*² of 0.86. The artificial data generated for the 7 missing days of OM samples were used in the PMF model. It was felt that this was superior to using the median OM concentration for the missing data period as suggested in the PMF user guide.

Meteorological data at the BORTAS-B DGS was collected every 15 min using a Davis Vantage Pro II weather station (Davis Instruments Corp. Hayward, California 94545 USA). The Davis Vantage Pro II weather sensors included wind speed, wind direction,

Identifying sources driving observed PM_{2.5} variability

M. D. Gibson et al.

Title Page

Abstract

Introduction

Conclusions

References

Tables

Figures

◀

▶

◀

▶

Back

Close

Full Screen / Esc

Printer-friendly Version

Interactive Discussion



**Identifying sources
driving observed
PM_{2.5} variability**

M. D. Gibson et al.

Title Page

Abstract

Introduction

Conclusions

References

Tables

Figures

◀

▶

◀

▶

Back

Close

Full Screen / Esc

Printer-friendly Version

Interactive Discussion



temperature, pressure, solar radiation, UV radiation, relative humidity and precipitation. The meteorological data was integrated to match the 24-h filter based sampling. The descriptive statistics of the meteorological variables that cover the PM_{2.5} sampling period at the BORTAS-B DGS are provided in Table 1. The average wind vector coinciding with each 24-h PM_{2.5} sample was determined using WRPLOT View (Lakes Environmental, Waterloo, Ontario, N2V 2A9, Canada). The daily wind vectors and the apportioned source masses were used to generate the source contribution rose shown in Fig. 9.

In addition, Environment Canada used the meteorological data from Halifax International airport to provide an overview of meteorological conditions within the Halifax Regional Municipality during the 45 days of filter sampling at the BORTAS-B DGS. A climatology review of synoptic meteorology patterns over Maritime Canada indicates a general west to east progression of transport flow. The period of the filter-based measurements at the DGS in summer 2011 was influenced by numerous weak low pressure systems during the first half of the sampling period (to 4 August). These systems, along with onshore moist southerly air flows provided extended periods with low level clouds and occasional periods of rain, drizzle and fog. Low cloud tends to inhibit photochemistry and promote aqueous-phase production of sulphate. Precipitation favors removal of particles from the atmosphere. Of the 45 sampling days, 13 had periods with sunny skies (6 + h). Ten of these days were in the latter portion of the sampling period, from 6 August onward, indicating limited photochemistry in the first portion of the sample period. Wind speed was significant (8.0 ms⁻¹ or more) on 7 days with 20 August being the windiest. Rain with amounts > 0.2 mm occurred on 16 days with 3 days (20 July, 2 August, 8 August) when amounts were greater than 20 mm. The 2 August rain event was due to a nearly stationary line of thunderstorms that developed over Halifax in the late afternoon. The line of thunderstorms did not move east of the area until the early hours of 3 August after providing 60 + mm of rain. A daily climatology review prepared by Environment Canada is presented in Table 2. These data was accessed via: http://www.climate.weatheroffice.gc.ca/climateData/canada_e.html.

3 Models

The HYbrid Single-Particle Lagrangian Integrated Trajectory (HYSPLIT) model was used to investigate the source regions of PM_{2.5} measured at the DGS during BORTAS-B. Figure 2 shows 2-day ensemble air mass back trajectories for the Halifax DGS during BORTAS-B we generated using HYSPLIT (Draxler and Rolph, 2012; Rolph, 2012). Two trajectories were obtained for each 24-h sampling period (07:00 UTC and 19:00 UTC). The HYSPLIT default of 950 hPa (500 m) was chosen as the arrival height to avoid trajectories hitting the ground before they arrive at the DGS. The mean location of the trajectory over the 2-day travel time was used to group the trajectories into four clusters: (1) N (315° to 45°), (2) marine (45° to 235°), (3) SW (235° to 265°), and (4) W-NW (265° to 315°). These clusters were chosen to reflect known source regions in Central Canada, Atlantic Canada and the North East United States, e.g. trajectory clusters coloured cyan are clearly under the influence of marine aerosol, the SW cluster (red) covers the Ohio valley, the interstate-95 corridor and other source regions in the NE US (Jeong et al., 2011; Dabek-Zlotorzynska et al., 2011). The NW cluster (green) covers the Windsor–Québec corridor, which is the population and industrial core of Central Canada and, as such, a major source region of secondary inorganic species and secondary OM (Jeong et al., 2011; Dabek-Zlotorzynska et al., 2011). The N cluster (blue) is a region of low anthropogenic emissions and should represent fairly clean air parcels impacting Halifax. Figure 3 shows the altitudes of these back trajectories, which we use to partition between the boundary layer (2 km) and free troposphere (> 2 km) en route to Halifax. These back trajectories will be discussed further in the results section.

The US EPA Positive Matrix Factorization (PMF) receptor model v3 was used for source apportionment of the PM_{2.5} sampled during BORTAS-B in Halifax. PMF method has an extensive heritage, having been applied to many PM_{2.5} source apportionment studies (Gugamsetty et al., 2012; Paatero, 1997; Paatero and Trapper, 1994; Henry, 1997; Martello et al., 2008; Jeong et al., 2008, 2011; Kim et al., 2004; Chen et al., 2007b; Brown et al., 2007; Larson et al., 2004; Song et al., 2001; Bari et al., 2009). The

ACPD

13, 4491–4533, 2013

Identifying sources driving observed PM_{2.5} variability

M. D. Gibson et al.

Title Page

Abstract

Introduction

Conclusions

References

Tables

Figures

◀

▶

◀

▶

Back

Close

Full Screen / Esc

Printer-friendly Version

Interactive Discussion



PMF model uses a mass balance equation, Eq. (1), that can be written to account for all m chemical species in the n samples as contributions from p independent sources (Hopke, 1991).

$$\chi_{ij} = \sum_{k=1}^p f_{ik} g_{kj} \quad (1)$$

5 where χ_{ij} is the i th elemental concentration measured in the j th sample, f_{ik} is the gravimetric concentration (ng mg^{-1}) from the i th element in the material from the k th source, and g_{kj} is the airborne $\text{PM}_{2.5}$ mass concentration (mg m^{-3}) of material from the k th source contributing to the j th sample. The following physical constraints are applied to the PMF model: (1) the model must fit the original data, (2) no negative source contributions are allowed and (3) the sum of the source contributions must be less than or equal to the total mass measured (Hopke, 1991). PMF then uses factor analysis to estimate the number and composition of the sources as well as their contribution to the total $\text{PM}_{2.5}$ mass. A priori knowledge of sources, meteorology and the chemical markers present in each PMF factor is used to identify the source associated with each factor (e.g. factors containing K and BC are likely associated with biomass burning). Correlation matrices and principal component analysis of the $\text{PM}_{2.5}$ mass, $\text{PM}_{2.5}$ chemical species, associated volatile organic compounds (VOCs), other gas measurements, air mass back trajectory models and other meteorological variables are often used to aid the identification of the source of the chemical species in each PMF factor (Jeong et al., 2011; Martello et al., 2008).

20 The task of PMF is to determine the loss function (Q), defined in Eq. (2), as follows:

$$Q = \sum_{i=1}^n \sum_{j=1}^m \left(\frac{e_{ij}}{S_{ij}} \right)^2 \quad (2)$$

where e_{ij} residual matrix of the i th element measured in the j th sample, S_{ij} is the uncertainty in the i th element measured in the j th sample. The loss function, Q , should

Identifying sources driving observed $\text{PM}_{2.5}$ variability

M. D. Gibson et al.

Title Page

Abstract

Introduction

Conclusions

References

Tables

Figures

◀

▶

◀

▶

Back

Close

Full Screen / Esc

Printer-friendly Version

Interactive Discussion



**Identifying sources
driving observed
PM_{2.5} variability**

M. D. Gibson et al.

Title Page

Abstract

Introduction

Conclusions

References

Tables

Figures

◀

▶

◀

▶

Back

Close

Full Screen / Esc

Printer-friendly Version

Interactive Discussion



be approximately equal to the degrees of freedom (Martello et al., 2008). When the calculated Q value is below the degrees of freedom then the uncertainty in the overall model fit is smaller than would be expected from random error, providing confidence that the data set is well defined by the model solution (Martello et al., 2008). When calculating Q , PMF ensures that all the species profiles (matrix F) are non-negative and that each source contribution to the PM_{2.5} mass is positive (matrix G). The PMF model simultaneously changes the elements of G and F in iterative steps to minimise Q . The procedure of Polissar et al. (1998) was used to determine each species measurement uncertainty based upon one-sigma analytical uncertainty values and minimum detection limits. The sum of the analytical uncertainty and one-third of the detection limit value was used as the overall uncertainty assigned to each measured concentration. Any component found to have a high signal-to-noise ratio were down-weighted as described by Paatero and Hopke (2003). The total PM_{2.5} mass values were down-weighted to weak as described in the PMF user guide (Eberly, 2005).

For the model base run, twenty random PMF initializations were conducted. Once the base run was completed the scatter plots and times series of the modelled and observed PM_{2.5} species were scrutinised with outliers being investigated. The normality of the model scaled residuals for each PM_{2.5} species was also scrutinized. Any PM_{2.5} species scaled residuals found to be ± 3 from zero were investigated further for poor model fit. Two checks on model performance were then made, bootstrapping and the PMF FPeak function. To fine tune the model the FPeak function within PMF was used to robustly minimise the effect of outliers. However, FPeak failed to improve the model and so was set to zero. The G-Space function was used to also check for model performance with no issues found with any of the species bi-plots. Once confidence in the model was achieved the PMF factor profiles were allocated a “source name” based upon the factor loadings of the key chemical markers present.

Chemical markers are used to help identify sources within the PMF source profiles, e.g. biomass burning has a number of characteristic chemical markers, e.g. potassium, BC and levoglucosan (1,6-anhydro- β -D-glucopyranose) (Bergauff et al., 2010; Ward

**Identifying sources
driving observed
PM_{2.5} variability**

M. D. Gibson et al.

Title Page

Abstract

Introduction

Conclusions

References

Tables

Figures

◀

▶

◀

▶

Back

Close

Full Screen / Esc

Printer-friendly Version

Interactive Discussion



et al., 2012; Jeong et al., 2008). Potassium is our preferred marker of long-range wildfire smoke plumes as it is conserved from source to receptor. Levoglucosan is a good marker for local biomass burning, but it is readily oxidized to 17 % of its original primary mass after 3.5 h of exposure to hydroxyl radicals (OH) (Hennigan et al., 2011), which reduces its ability to identify Long Range Transport (LRT) of biomass burning. However, internally mixed Levoglucosan may not be oxidized, being protected by the outer layer of the particulate, and so may still be useful as a marker of LRT Boreal wildfire burning (Hennigan et al., 2011). Robust chemical markers of ship emissions include sulfate (SO₄), vanadium (V), nickel (Ni) and BC (Hobbs et al., 2000; Isakson et al., 2001; Zhao et al., 2013). V/Ni ratios originating from heavy fuel oil (HFO) used in ships range from 1.9–6.5 (Zhao et al., 2013). The sulphur content of HFO is currently between 1.0 % and 3.5 %, and during combustion produces particulate SO₄ (Lack et al., 2011). Ship emissions also contain large quantities of BC particulate (Lack and Corbett, 2012). Unambiguous markers of fugitive surficial dust include iron (Fe), aluminium (Al), calcium (Ca) and silicon (Si) (Jeong et al., 2011; Martello et al., 2008; Gugamsetty et al., 2012). Primary sea salt markers include sodium (Na), chloride (Cl), magnesium (Mg), and Ca (Gibson et al., 2009) and Na, Ca, Mg and nitrate (NO₃) for aged marine secondary aerosol (Jeong et al., 2011; Gibson et al., 2009). Nitrate, ammonium (NH₄) and SO₄ are markers of long-range secondary inorganic PM produced by photochemical reactions of pre-cursor gases NO₂, SO₂ and ammonia (NH₃) (Yin and Harrison, 2008; Gibson et al., 2009). Chemical markers for vehicular emissions include BC, bromine (Br), antimony (Sb), manganese (Mn), and Fe (Larson et al., 2004; Huang et al., 1994). Copper (Cu), barium (Ba) and Fe are markers for vehicle brake wear (Harrison et al., 2011; Bukowiecki et al., 2010; Chen et al., 2007a) and zinc (Zn) and cadmium (Cd) are markers for vehicle tire wear (Bukowiecki et al., 2010; Olajire and Ayodele, 1997; Chen et al., 2007a). Diesel emissions have been previously characterized by high PMF loading of PM_{2.5} mass and BC (Martello et al., 2008; Chen et al., 2007a). Selenium (Se) is often used as a good marker for coal combustion (Chow et al., 2004). The source chemical profiles contained in the US EPA Speciate database provide additional ev-

idence to identify source chemical markers in PMF chemical species factor profiles (Ward et al., 2012; Jaeckels et al., 2007).

4 Results and discussion

4.1 HYSPLIT cluster analysis

5 Figure 2 shows using the ensemble HYSPLIT, 2-day, air mass back trajectories that 40% of the air masses entering Halifax during the BORTAS-B PM_{2.5} sampling campaign originated from the marine sector, 16% from the SW (NE US), 27% from the WNW (Windsor–Quebec source region) and 16% from the N. Figure 3 shows that
10 air mass back trajectories from all four clusters have a high likelihood that the trajectory profiles were in the boundary layer during the previous 48 h. Our analysis also showed that over 80% of the back trajectories were below 1.5 km for the entire 48 h. The profiles from the N (blue) show the highest probability of air subsiding from the free troposphere; however, we expect these profiles to be associated with clean air regardless of the altitude of the back trajectories. The Marine cluster mostly originate
15 from the boundary layer, as expected (Holzinger et al., 2007). Of the two potentially polluted clusters shown in Fig. 3, the SW cluster and WNW cluster appear to be mainly associated with boundary layer flow.

4.2 Descriptive statistics

20 Table 3 provides the descriptive statistics for the PM_{2.5} species and associated meteorological variables sampled during BORTAS-B. The median PM_{2.5} concentration is 3.9 µg m⁻³, which is considerably lower than historical (2006–2008) summer time value (median 9.0 µg m⁻³) measured at the NAPS station in down town Halifax and reported by Jeong et al. (2011). The difference between these two values might be due to greater vehicle density in the downtown core of Halifax compared to the BORTAS-B DGS in

Identifying sources driving observed PM_{2.5} variability

M. D. Gibson et al.

Title Page

Abstract

Introduction

Conclusions

References

Tables

Figures



Back

Close

Full Screen / Esc

Printer-friendly Version

Interactive Discussion



Identifying sources driving observed PM_{2.5} variability

M. D. Gibson et al.

Title Page

Abstract

Introduction

Conclusions

References

Tables

Figures

◀

▶

◀

▶

Back

Close

Full Screen / Esc

Printer-friendly Version

Interactive Discussion



the more residential south end of Halifax. Unfortunately, the Federal Government PM_{2.5} monitoring in downtown Halifax during BORTAS-B was too sparse to make any direct comparison with our data possible. The BORTAS-B PM_{2.5} median is also considerably lower than summertime median PM_{2.5} concentrations found in Toronto (12 µg m⁻³) and Windsor, Canada (15 µg m⁻³) (Jeong et al., 2011), which we attribute to the significantly lower population, vehicle and industrial density in Halifax in comparison to these other Canadian cities. In addition, with reference to Table 2, precipitation amounts > 0.2 mm occurred on 16 days, with two days (2 August and 8 August) when amounts were greater than 20 mm. The significant precipitation occurring during roughly half of the sampling period helps explain the reduced average PM_{2.5} concentrations observed during BORTAS-B when compared with previous years. Despite the low PM_{2.5} sample mass, the key chemical species needed to conduct PMF modelling were above the limit of detection (LOD).

4.3 PM_{2.5} composition

Figures 4–7 show time series of daily major, macro, minor and trace PM_{2.5} components together with the total PM_{2.5} mass concentration. The main contributing species seen during the relatively low PM_{2.5} concentrations observed between 13 July and 15 July were Na and Cl (indicative of Sea Salt) as well as some OM and BC (local combustion emissions; also, filter absorption can be affected by other absorbers, such as brown carbon, and at 880 nm by scattering due to larger particles of sea salt), with greatly reduced, or absent, NH₄, SO₄, NO₃, Se and Pb (indicative of LRT pollution), compared to other time periods. The air mass back trajectories during this low PM_{2.5} mass period were from the north, a region of low primary and secondary PM_{2.5} emission, thus providing evidence to explain the low concentrations experienced on 13 July and 15 July. Between 16 July and 24 July there was a PM_{2.5} episode as shown by Fig. 4. Figures 4 and 5 show that the dominant species during this period were BC, NH₄, S, SO₄, NO₃ and OM with input from Se and Pb, as shown in Fig. 7. The presence of

elevated Ni, V and SO₄ suggest ship emissions as the probable source contributing to the PM_{2.5} mass on this day (Zhao et al., 2013).

4.4 PMF receptor modelling

The number of factors (sources) that PMF could apportion were explored in an iterative process from 5 factor profiles through to 15 factor profiles. The number of factors chosen was based on the high factor loadings of key chemical markers, the ensemble HYSPLIT trajectory clusters (Fig. 2), wind roses analysis and a priori knowledge of known sources impacting Halifax. The seven factors chosen were LRT Pollution (LRTP), LRT Pollution Marine Mixture (LRTPMM), Refinery, Ship Emissions, Vehicles, Fugitive Dust and Sea Salt which were anticipated by the individual chemical markers related to these sources as discussed in Sect. 4.3. High factor loadings of OM, PM_{2.5}, SO₄, S and NH₄ were used to identify LRTP. High factor loadings of OM, NO₃ and Na were used to identify LRTPMM. The LRTPMM is likely a mixture of aerosol pollution outflow from the NE US and Sea Salt that has undergone Cl loss via reactions with acidic aerosol (Gibson et al., 2009; Leaitch et al., 1996; Calvert et al., 1985). The presence of NO₃ in the LRTPMM could also be attributed to night-time reactions of NO₂ with O₃, with NO₃ also reacting with sea salt to remove Cl (Finlayson-Pitts and Pitts, 1999; Calvert et al., 1985). The Refinery factor was identified by the presence of Pb, Zn, Cu, Cr and V (Jeong et al., 2011). Ship Emissions were identified by the high factor loadings of Ni, V, BC and SO₄ (Zhao et al., 2013). Vehicles were identified by the high factor loadings of BC, OM, Ba, Cu, Br and Zn (Gietl et al., 2010). It was not possible with this data set to split the vehicle factors into gasoline or diesel emissions, brakes or tire wear sources. Fugitive Dust was identified by high factor loadings for Al, Ca, K, Fe and Si (Jeong et al., 2011). Sea Salt was identified from the high factor loadings for Na, Cl, 55 % and 88 % respectively, which is the same ratio as found in sea water (Gibson et al., 2009). Although Sea Salt was observed in all PMF factor iterations, 5 through 15, the mass contribution was so low that PMF failed to apportion mass to any of the PMF model runs. This is perhaps not surprising given the very low PM_{2.5} mass observed

Identifying sources driving observed PM_{2.5} variability

M. D. Gibson et al.

Title Page

Abstract

Introduction

Conclusions

References

Tables

Figures



Back

Close

Full Screen / Esc

Printer-friendly Version

Interactive Discussion



during BORTAS-B and the fact that Sea Salt PM are mostly associated with the coarse size fraction. However, there was evidence of a contribution of aged marine aerosol (as indicated by the presence of Na and NO₃ markers) to the LRTPMM source coincident with airflow from the NE US and crossing the ocean en route to Halifax (Leitch et al., 1996). Therefore, the PMF receptor model apportioned six PM_{2.5} sources. Figure 8 presents a time series of the six contributing sources to PM_{2.5} mass estimated using PMF during BORTAS-B.

Figure 9 shows the local wind directional dependence of the PM_{2.5} source contributions estimated by PMF. Ship emission PM_{2.5} source contribution aligns with the cruise ship terminal, harbour shipping lane and Naval base with little ship emission contribution directly to WNW, which is in the opposite direction to the harbour. Figure 9 confirms that ship emissions were correctly allocated to the PMF factor profile. Figure 8 shows that between 13 July and 16 July the main contributing PM_{2.5} source were Vehicles, which can be explained by the N and NW wind directions (Table 2) aligned with the highways directly upwind of the DGS. The Fugitive Dust source is most probably associated with immediate local surficial material re-suspension (Harrison et al., 2011). From Fig. 9., we found that the Fugitive Dust was associated with a westerly wind direction. This wind direction is coincident with the major street landscaping that occurred directly below the western side of the DGS throughout BORTAS-B. It was found that the Refinery Source does not appear to have a strong local wind directional dependence. The refinery is on the other side of Halifax harbour so that the local wind direction is less appropriate than for more immediate local sources such as vehicles and fugitive dust. Air mass back trajectory analysis did not yield any further insight into wind direction dependence for the refinery source. Marine inversions and the complexity of the harbour and city topography that lay between the refinery and the DGS may have perturbed any wind directional dependence for this source.

Figure 10 shows the PMF source contribution for LRTP and LRTPMM associated with the SW and W air mass back trajectories. The back trajectories associated with the days with high loadings of LRTP have all passed over eastern Canada or the NE

Identifying sources driving observed PM_{2.5} variability

M. D. Gibson et al.

Title Page

Abstract

Introduction

Conclusions

References

Tables

Figures

◀

▶

◀

▶

Back

Close

Full Screen / Esc

Printer-friendly Version

Interactive Discussion



US (Fig. 10). This is the region where we expect the largest sulphur sources. The days with high loadings of LRTPMM (Fig. 10) have more variability. While the trajectories generally come from the W, several of the back trajectories have primarily been over the ocean for most of the 48-h. The presence of Na and the loss of Cl associated with the LRTPMM source suggests continental acidic aerosol outflow mixing with marine aerosol en route to Halifax (Holzinger et al., 2007; Sirois and Bottenheim, 1995; Gibson et al., 2009; Leaitch et al., 1996).

Figure 11 shows the average mass and (percentage) contribution from the six sources estimated by PMF during BORTAS-B. The Refinery contribution of $0.081 \mu\text{g m}^{-3}$ (2.2 %) during BORTAS-B is somewhat lower than $0.3 \mu\text{g m}^{-3}$ (3.5 %) obtained by PMF conducted by Jeong et al. (2011) (Jeong-PMF). The comparison for the BORTAS-B PMF vehicles with Jeong-PMF vehicle $\text{PM}_{2.5}$ mass contribution was $0.49 \mu\text{g m}^{-3}$ (13.2 %) and $1.0 \mu\text{g m}^{-3}$ (14.2 %) respectively which is very similar in terms of % contribution but half the $\text{PM}_{2.5}$ mass seen during BORTAS-B. The comparison between the BORTAS-B PMF and Jeong-PMF for the Ship Emission was $0.13 \mu\text{g m}^{-3}$ (3.4 %) and $0.6 \mu\text{g m}^{-3}$ (9.1 %) respectively, showing a 4.6 times mass reduction and 3 times reduction in % contribution between the previous PMF study conducted on 2006–2008 data and the BORTAS-B study. This could be due to the reduction in the sulphur content (3.5 % to 1 %) of HFO used in ships in the intervening period between these two studies which, coincidentally, is the same ratio of sulphur reduction in HFO as the $\text{PM}_{2.5}$ mass reduction seen in the BORTAS-B study. The comparison between BORTAS-B PMF and Jeong-PMF Fugitive Dust is $0.23 \mu\text{g m}^{-3}$ (6.3 %) and $0.3 \mu\text{g m}^{-3}$ (3.8 %) respectively, both are similar in magnitude for $\text{PM}_{2.5}$ mass but with a 39 % greater contribution to $\text{PM}_{2.5}$ during BORTAS-B. The fugitive dust contribution during BORTAS-B can be explained by street landscaping and exterior building restoration work that occurred during BORTAS-B. The comparison between BORTAS-B PMF and Jeong-PMF for the LRTP was $1.75 \mu\text{g m}^{-3}$ (47 %) and $2.6 \mu\text{g m}^{-3}$ (37.3 %), which are similar in magnitude; providing confidence in the BORTAS-B PMF results. In a comparison between BORTAS-B PMF LRTPMM and Jeong-PMF LRTPMM, Jeong

Identifying sources driving observed $\text{PM}_{2.5}$ variability

M. D. Gibson et al.

Title Page

Abstract

Introduction

Conclusions

References

Tables

Figures

◀

▶

◀

▶

Back

Close

Full Screen / Esc

Printer-friendly Version

Interactive Discussion



Identifying sources driving observed PM_{2.5} variability

M. D. Gibson et al.

Title Page

Abstract

Introduction

Conclusions

References

Tables

Figures

◀

▶

◀

▶

Back

Close

Full Screen / Esc

Printer-friendly Version

Interactive Discussion



et al. (2011) estimated that secondary NO₃ aerosol in Halifax was 1.0 μg m⁻³ (27.9 %) and 0.7 μg m⁻³ (9.3 %), which is again similar in mass contribution to BORTAS-B but roughly three times the % contribution when compared to the Jeong-PMF results. The factor associated with “unaltered” sea salt was identified in the BORTAS-B samples but there was too little mass for PMF to apportion, although aged marine aerosol did contribute to the LRTPMM source. The Jeong-PMF reported a Sea Salt contribution of 1.3 μg m⁻³ (18.3 %) contribution to PM_{2.5} mass in Halifax, however this was an average over 2 yr and include all seasons (Jeong et al., 2011).

The sum of the masses associated with the six apportioned sources obtained from PMF were compared with the original total PM_{2.5} mass. The bias of the PMF model was calculated as $(A - T)/T$, where A is the PMF PM_{2.5} mass concentration and T is observed PM_{2.5} mass concentration over the 45 days of sampling. The root-mean-square error (RMSE) was used to determine the accuracy of the PMF model, Eq. (3).

$$\text{RMSE} = \sqrt{\frac{1}{n} \sum_{i=1}^n (\hat{y}_i - y_i)^2} \quad (3)$$

where \hat{y} = PMF model total PM_{2.5} mass concentration and y = observed total PM_{2.5} mass concentration with units expressed in μg m⁻³.

Linear regression of the PMF model versus observed PM_{2.5} mass yielded a slope of 0.874, intercept of 1.24 and $r^2 = 0.87$. The PMF model bias = 0.17 and the RSME = 1.5 μg m⁻³, showing that the PMF model skill was high.

5 Conclusion

The PMF model was used to determine six major sources contributing to the PM_{2.5} mass sampled during the BORTAS-B study. Although other BORTAS-B related observations (Palmer, 2013) showed that transient Boreal wildfire smoke plumes did pass

**Identifying sources
driving observed
PM_{2.5} variability**

M. D. Gibson et al.

Title Page

Abstract

Introduction

Conclusions

References

Tables

Figures

◀

▶

◀

▶

Back

Close

Full Screen / Esc

Printer-friendly Version

Interactive Discussion



over and impact the surface in Halifax, there was insufficient mass for PMF to apportion. However, this study does provide valuable new insight into the major local and distant sources contributing to surface PM_{2.5} mass at the DGS during BORTAS-B. It was shown that the dominant source contribution to summertime PM_{2.5} mass in Halifax was from LRT Pollution with a contribution from aged marine aerosol (75%) coincident with SW air flow. This is consistent with the conventional wisdom that Nova Scotia is the “tail pipe of North America”. Comparison of the PMF total PM_{2.5} mass with the observed total PM_{2.5} mass over the sampling period showed good agreement ($r^2 = 0.87$, bias = 0.17 and RSME = $1.5 \mu\text{g m}^{-3}$), demonstrating the PMF receptor model performed well. The study highlights the utility of using air mass back trajectories coupled with local wind direction dependence to help identify the source of PM_{2.5}. The techniques used in this study show considerable promise for further application to other sites and to identify other source categories of PM_{2.5}. This study provides new data that will be useful for other BORTAS-B related investigations as well as new information that can be used for population air pollution exposure assessment, air quality management and urban planning in Halifax.

Acknowledgements. We are grateful to Paul Palmer (University of Edinburgh) for funding project consumables via his Philip Leverhulme Prize. We would like to thank Health Canada for the loan of the Magee black carbon Aethalometer, Thermo ChemComb samplers, filter weighing and XRF analysis. Many thanks to CD-NOVA for the loan of the Thermo Partisol 2025-Dichotomous sampler. Gratitude to Heather Daurie, Department of Civil and Resources Engineering, Dalhousie University for analysing the water soluble metals species. We acknowledge the support of Environment Canada and Nova Scotia Environment, Air Quality Section, for the provision of comparative air pollution data, meteorological data and general support and advice.

References

- Allen, R. W., Mar, T., Koenig, J., Liu, L. J. S., Gould, T., Simpson, C., and Larson, T.: Changes in lung function and airway inflammation among asthmatic children residing in a woodsmoke-impacted urban area, *Inhal. Toxicol.*, 20, 423–433, 2008.
- 5 Babu, S. S. and Moorthy, K. K.: Aerosol black carbon over a tropical coastal station in India, *Geophys. Res. Lett.*, 29, 13-11-13-14, doi:10.1029/2002GL015662, 2002.
- Bari, M. A., Baumbach, G., Kuch, B., and Scheffknecht, G.: Wood smoke as a source of particle-phase organic compounds in residential areas, *Atmos. Environ.*, 43, 4722–4732, doi:10.1016/j.atmosenv.2008.09.006, 2009.
- 10 Bergauff, M. A., Ward, T. J., Noonan, C. W., Migliaccio, C. T., Simpson, C. D., Evanski, A. R., and Palmer, C. P.: Urinary levoglucosan as a biomarker of wood smoke: results of human exposure studies, *J. Expo. Sci. Env. Epid.*, 20, 385–392, 2010.
- Brown, S. G., Frankel, A., and Hafner, H. R.: Source apportionment of VOCs in the Los Angeles area using positive matrix factorization, *Atmos. Environ.*, 41, 227–237, doi:10.1016/j.atmosenv.2006.08.021, 2007.
- 15 Bukowiecki, N., Lienemann, P., Hill, M., Furger, M., Richard, A., Amato, F., Prévôt, A. S. H., Baltensperger, U., Buchmann, B., and Gehrig, R.: PM₁₀ emission factors for non-exhaust particles generated by road traffic in an urban street canyon and along a freeway in Switzerland, *Atmos. Environ.*, 44, 2330–2340, doi:10.1016/j.atmosenv.2010.03.039, 2010.
- 20 Calvert, J. G., Lazrus, A., Kok, G. L., Heikes, B. G., Walega, J. G., Lind, J., and C. A. Cantrell: Chemical mechanisms of acid generation in the troposphere, *Nature*, 317, 27–35, 1985.
- Chen, F., Dimmick, F., Williams, R., and Baldauf, R.: Particulate matter concentration measurements from Near Road Studies (NRS) in Raleigh, North Carolina, 17th Annual Conference of the International Society for Exposure Analysis, Abstract No. 43, 14 October 2007, Durham, Research Triangle Park, North Carolina, 2007a.
- 25 Chen, L. W. A., Watson, J. G., Chow, J. C., and Magliano, K. L.: Quantifying PM_{2.5} source contributions for the San Joaquin Valley with multivariate receptor models, *Environ. Sci. Technol.*, 41, 2818–2826, doi:10.1021/es0525105, 2007b.
- Chow, J. C., Watson, J. G., Kuhns, H., Etyemezian, V., Lowenthal, D. H., Crow, D., Kohl, S. D., Engelbrecht, J. P., and Green, M. C.: Source profiles for industrial, mobile, and area sources in the big bend regional aerosol visibility and observational study, *Chemosphere*, 54, 185–208, doi:10.1016/j.chemosphere.2003.07.004, 2004.
- 30

Identifying sources driving observed PM_{2.5} variability

M. D. Gibson et al.

Title Page

Abstract

Introduction

Conclusions

References

Tables

Figures

◀

▶

◀

▶

Back

Close

Full Screen / Esc

Printer-friendly Version

Interactive Discussion



Identifying sources driving observed PM_{2.5} variability

M. D. Gibson et al.

Title Page

Abstract

Introduction

Conclusions

References

Tables

Figures

◀

▶

◀

▶

Back

Close

Full Screen / Esc

Printer-friendly Version

Interactive Discussion



- Dabek-Zlotorzynska, E., Dann, T. F., Martinelango, P. K., Celso, V., Brook, J. R., Mathieu, D., Ding, L., and Austin, C. C.: Canadian National Air Pollution Surveillance (NAPS) PM_{2.5} speciation program: methodology and PM_{2.5} chemical composition for the years 2003–2008, *Atmos. Environ.*, 45, 673–686, 2011.
- 5 Dominici, F., Peng, R. D., Bell, M. L., Pham, L., McDermott, A., Zeger, S. L., and Samet, J. M.: Fine particulate air pollution and hospital admission for cardiovascular and respiratory diseases, *J. Am. Med. Assoc.*, 295, 1127–1134, doi:10.1001/jama.295.10.1127, 2006.
- Draxler, R. R. and Rolph, G. D.: HYSPLIT (HYbrid Single-Particle Lagrangian Integrated Trajectory) model access via NOAA ARL READY Website, NOAA Air Resources Laboratory, Silver Spring, MD, 2012.
- 10 Eberly, S.: EPA PMF 1.1 User's Guide, US Environmental Protection Agency National Exposure Research Laboratory Research Laboratory Triangle Park, NC 27711, available at: http://www.epa.gov/heasd/products/pmf/EPAPMF3.0UserGuidev16_092208_final.pdf (last access: 11 January 2013), 2005.
- 15 Finlayson-Pitts, B. J. and Pitts, J. N.: *Chemistry of the Upper and Lower Atmosphere*, Academic Press, an Imprint of Elsevier, USA, ISBN: 0-12-257060-x, 2000.
- Gambaro, G., Zangrando, R., Gabrielli, P., Barbante, C., and Cescon, P.: Direct determination of levoglucosan at the picogram per milliliter level in Antarctic ice by High-Performance Liquid Chromatography/Electrospray Ionization Triple Quadrupole Mass Spectrometry, *Anal. Chem.*, 80, 1649–1655, 2008.
- 20 Gibson, M. D., Heal, M. R., Bache, D. H., Hursthouse, A. S., Beverland, I. J., Craig, S. E., Clark, C. F., Jackson, M. H., Guernsey, J. R., and Jones, C.: Using mass reconstruction along a four-site transect as a method to interpret PM₁₀ in West-Central Scotland, UK, *J. Air Waste Manag.*, 59, 1429–1436, 2009.
- 25 Gietl, J. K., Lawrence, R., Thorpe, A. J., and Harrison, R. M.: Identification of brake wear particles and derivation of a quantitative tracer for brake dust at a major road, *Atmos. Environ.*, 44, 141–146, 2010.
- Gugamsetty, B., Wei, H., Liu, C. N., Awasthi, A., Hsu, S. C., Tsai, C. J., Roam, G. D., Wu, Y. C., and Chen, C. F.: Source characterization and apportionment of PM₁₀, PM_{2.5} and PM_{0.1} by using positive matrix factorization, *Aerosol Air Qual. Res.*, 12, 476–491, 2012.
- 30 Hansen, A. D. A.: *The Aethalometer*, Magee Scientific Company, Berkeley, California, USA, 1–209, 2005.

**Identifying sources
driving observed
PM_{2.5} variability**

M. D. Gibson et al.

Title Page

Abstract

Introduction

Conclusions

References

Tables

Figures

◀

▶

◀

▶

Back

Close

Full Screen / Esc

Printer-friendly Version

Interactive Discussion



Harrison, R. M., Beddows, D. C. S., and Dall'Osto, M.: PMF analysis of wide-range particle size spectra collected on a major highway, *Environ. Sci. Technol.*, 45, 5522–5528, doi:10.1021/es2006622, 2011.

Hennigan, C. J., Miracolo, M. A., Engelhart, G. J., May, A. A., Presto, A. A., Lee, T., Sullivan, A. P., McMeeking, G. R., Coe, H., Wold, C. E., Hao, W.-M., Gilman, J. B., Kuster, W. C., de Gouw, J., Schichtel, B. A., Collett Jr., J. L., Kreidenweis, S. M., and Robinson, A. L.: Chemical and physical transformations of organic aerosol from the photo-oxidation of open biomass burning emissions in an environmental chamber, *Atmos. Chem. Phys.*, 11, 7669–7686, doi:10.5194/acp-11-7669-2011, 2011.

Henry, R. C.: History and fundamentals of multivariate air quality receptor models, *Chemometr. Intell. Lab.*, 37, 525–530, 1997.

Hobbs, P. V., Garrett, T. J., Ferek, R. J., Strader, S. R., Hegg, D. A., Frick, G. M., Hoppel, W. A., Gasparovic, R. F., Russell, L. M., Johnson, D. W., O'Dowd, C., Durkee, P. A., Nielson, K. E., and Innis, G.: Emissions from ships with respect to their effects on clouds, *J. Atmos. Sci.*, 57, 2570–2590, 2000.

Holzinger, R., Millet, D. B., Williams, B., Lee, A., Kreisberg, N., Hering, S. V., Jimenez, J., Allan, J. D., Worsnop, D. R., and Goldstein, A. H.: Emission, oxidation, and secondary organic aerosol formation of volatile organic compounds as observed at Chebogue Point, Nova Scotia, *J. Geophys. Res.*, 112, D10S24, doi:10.1029/2006jd007599, 2007.

Hopke, P. K.: An introduction to Receptor Modeling, *Chemometr. Intell. Lab.*, 10, 21–43, 1991.

Huang, X., Olmez, I., Aras, N. K., and Gordon, G. E.: Emissions of trace elements from motor vehicles: Potential marker elements and source composition profile, *Atmos. Environ.*, 28, 1385–1391, doi:10.1016/1352-2310(94)90201-1, 1994.

Isakson, J., Persson, T. A., and Lindgren, E. S.: Identification and assessment of ship emissions and their effects in the harbour of Goteborg, Sweden, *Atmos. Environ.*, 35, 3659–3666, 2001.

Jaekels, J. M., Bae, M.-S., and Schauer, J. J.: Positive Matrix Factorization (PMF) analysis of molecular marker measurements to quantify the sources of organic aerosols, *Environ. Sci. Technol.*, 41, 5763–5769, doi:10.1021/es062536b, 2007.

Jeong, C.-H., Evans, G. J., Dann, T., Graham, M., Herod, D., Dabek-Zlotorzynska, E., Mathieu, D., Ding, L., and Wang, D.: Influence of biomass burning on wintertime fine particulate matter: source contribution at a valley site in rural British Columbia, *Atmos. Environ.*, 42, 3684–3699, 2008.

Identifying sources driving observed PM_{2.5} variability

M. D. Gibson et al.

Title Page

Abstract

Introduction

Conclusions

References

Tables

Figures

◀

▶

◀

▶

Back

Close

Full Screen / Esc

Printer-friendly Version

Interactive Discussion



- Jeong, C.-H., McGuire, M. L., Herod, D., Dann, T., Dabek-Zlotorzynska, E., Wang, D., Ding, L., Celo, V., Mathieu, D., and Evans, G.: Receptor model based identification of PM_{2.5} sources in Canadian cities, *Atmos. Pollut. Res.*, 2, 158–171, doi:10.5094/APR.2011.021, 2011.
- Kim, E., Hopke, P. K., and Edgerton, E. S.: Improving source identification of Atlanta aerosol using temperature resolved carbon fractions in positive matrix factorization, *Atmos. Environ.*, 38, 3349–3362, 2004.
- Lack, D. A. and Corbett, J. J.: Black carbon from ships: a review of the effects of ship speed, fuel quality and exhaust gas scrubbing, *Atmos. Chem. Phys.*, 12, 3985–4000, doi:10.5194/acp-12-3985-2012, 2012.
- Lack, D. A., Cappa, C. D., Langridge, J., Bahreini, R., Buffaloe, G., Brock, C., Cerully, K., Coffman, D., Hayden, K., Holloway, J., Lerner, B., Massoli, P., Li, S.-M., McLaren, R., Middlebrook, A. M., Moore, R., Nenes, A., Nuaanan, I., Onasch, T. B., Peischl, J., Perring, A., Quinn, P. K., Ryerson, T., Schwartz, J. P., Spackman, R., Wofsy, S. C., Worsnop, D., Xi-ang, B., and Williams, E.: Impact of fuel quality regulation and speed reductions on shipping emissions: implications for climate and air quality, *Environ. Sci. Technol.*, 45, 9052–9060, doi:10.1021/es2013424, 2011.
- Larson, T., Gould, T., Simpson, C., Liu, L. J., Claiborn, C., and Lewtas, J.: Source apportionment of indoor, outdoor, and personal PM_{2.5} in Seattle, Washington, using Positive Matrix Factorization, *J. Air Waste Manag.*, 54, 1175–1187, 2004.
- Lawless, P. A., Rodes, C. E., and Ensor, D. S.: Multiwavelength absorbance of filter deposits for determination of environmental tobacco smoke and black carbon, *Atmos. Environ.*, 38, 3373–3383, 2004.
- Leaïch, W. R., Banic, C. M., Isaac, G. A., Couture, M. D., Liu, P. S. K., Gultepe, I., Li, M. M., Klienman, L., Daum, P. H., and MacPherson, J. I.: Physical and chemical observations in marine stratus during the 1993 North Atlantic Regional Experiment: factors controlling cloud droplet number concentrations, *J. Geophys. Res.*, 101, 29123–29135, 1996.
- Liu, P. S. K., Deng, R., Smith, K. A., Williams, L. R., Jayne, J. T., Canagaratna, M. R., Moore, K., Onasch, T. B., Worsnop, D. R., and Deshler, T.: Transmission efficiency of an aerodynamic focusing lens system: comparison of model calculations and laboratory measurements for the aerodyne aerosol mass spectrometer, *Aerosol Sci. Technol.*, 41, 721–733, doi:10.1080/02786820701422278, 2007.
- Martello, D. V., Pekneya, N. J., Anderson, R. R., Davidson, C. I., Hopke, P. K., Kim, E., Christensen, W. F., Mangelson, N. F., and Eatough, D. J.: Apportionment of ambient pri-

Identifying sources driving observed PM_{2.5} variability

M. D. Gibson et al.

Title Page

Abstract

Introduction

Conclusions

References

Tables

Figures

◀

▶

◀

▶

Back

Close

Full Screen / Esc

Printer-friendly Version

Interactive Discussion

mary and secondary fine particulate matter at the Pittsburgh National Energy Laboratory particulate matter characterization site using Positive Matrix Factorization and a potential source contributions function analysis, *J. Air Waste Manag.*, 58, 357–368, doi:10.3155/1047-3289.58.3.357, 2008.

5 Maykut, N. N., Lewtas, J., Kim, E., and Larson, T. V.: Source apportionment of PM_{2.5} at an urban IMPROVE site in Seattle, Washington, *Environ. Sci. Technol.*, 37, 5135–5142, doi:10.1021/es030370y, 2003.

Ng, N. L., Herndon, S. C., Trimborn, A., Canagaratna, M. R., Croteau, P. L., Onasch, T. B., Sueper, D., Worsnop, D. R., Zhang, Q., Sun, Y. L., and Jayne, J. T.: An Aerosol Chemical Speciation Monitor (ACSM) for routine monitoring of the composition and mass concentrations of ambient aerosol, *Aerosol Sci. Technol.*, 45, 780–794, doi:10.1080/02786826.2011.560211, 2011.

Norris, G., Larson, T., Koenig, J., Claiborn, C., Sheppard, L., and Finn, D.: Asthma aggravation, combustion, and stagnant air, *Thorax*, 55, 466–470, 2000.

15 Olajire, A. A. and Ayodele, E. T.: Contamination of roadside soil and grass with heavy metals, *Environ. Int.*, 23, 91–101, doi:10.1016/s0160-4120(96)00080-3, 1997.

Paatero, P.: Least squares formulation of robust non-negative factor analysis, *Chemometr. Intell. Lab.*, 37, 23–35, 1997.

Paatero, P. and Trapper, U.: Positive Matrix Factorization: a non-negative factor model with optimal utilization of error estimates of data values, *Environmetrics*, 5, 111–126, 1994.

Paatero, P. and Hopke, P. K.: Discarding or downweighting high-noise variables in factor analytic models, 8th International Conference on Chemometrics and Analytical Chemistry, *Analytica Chimica Acta*, 490, 277–289, 2003.

25 Palmer, P. I., M. Parrington, Lee, J. D., Lewis, A. C., Rickard, A. R., Bernath, P. F., Duck, T. J., Waugh, D. L., Tarasick, D. W., Andrews, S., Aruffo, E., Bailey, L. J., Barrett, E., Bauquitte, S. J. B., Curry, K. R., Carlo, P. D., Chisholm, L., Dan, L., Drummond, J. R., Forster, G., Franklin, J. E., Gibson, M. D., Griffin, D., Helmig, D., Hopkins, J. R., Hopper, J. T., Jenkin, M. E., Kindred, D., Kliever, J., Breton, M. L., Matthiesen, S., Maurice, M., Moller, S., Moore, D. P., Oram, D. E., O'Shea, S. J., Owen, R. C., Pagnello, C. M. L. S., Pawson, S., Percival, C. J., Pierce, J. R., Punjabi, S., Purvis, R. M., Remedios, J. J., Rotermund, K. M., Sakamoto, K. M., Strawbridge, K. B., Strong, K., Taylor, J., Trigwell, R., Tereszchuk, K. A., Walker, K. A., Weaver, D., Whaley, C., and Young, J. C.: Quantifying the impact of BOREal forest fires on Tropospheric oxidants over the Atlantic using Aircraft and Satellites (BOR-

Identifying sources driving observed PM_{2.5} variability

M. D. Gibson et al.

Title Page

Abstract

Introduction

Conclusions

References

Tables

Figures

◀

▶

◀

▶

Back

Close

Full Screen / Esc

Printer-friendly Version

Interactive Discussion



TAS) experiment: design, execution and science overview, Atmos. Chem. Phys. Discuss., 13, 4127–4181, doi:10.5194/acpd-13-4127-2013, 2013.

Parrington, M., Palmer, P. I., Henze, D. K., Tarasick, D. W., Hyer, E. J., Owen, R. C., Helmig, D., Clerbaux, C., Bowman, K. W., Deeter, M. N., Barratt, E. M., Coheur, P.-F., Hurtmans, D., Jiang, Z., George, M., and Worden, J. R.: The influence of boreal biomass burning emissions on the distribution of tropospheric ozone over North America and the North Atlantic during 2010, Atmos. Chem. Phys., 12, 2077–2098, doi:10.5194/acp-12-2077-2012, 2012.

Polissar, A. V., Hopke, P. K., Paatero, P., Malm, W. C., and Sisler, J. F.: Atmospheric aerosol over Alaska: 1. Elemental composition and sources, J. Geophys. Res., 103, 19045–19057, 1998.

Pope, C. A., Burnett, R. T., Thun, M. J., Calle, E. E., Krewski, D., Ito, K., and Thurston, G. D.: Lung cancer, cardiopulmonary mortality, and long-term exposure to fine particulate air pollution, J. Am. Med. Assoc., 287, 1132–1141, doi:10.1001/jama.287.9.1132, 2002.

Rolph, G. D.: Real-time Environmental Applications and Display sYstem (READY), NOAA Air Resources Laboratory, Silver Spring, MD, 2012.

Sirois, A. and Bottenheim, J. W.: Use of backward trajectories to interpret the 5-yr record of PAN and O₃ ambient air concentrations at Kejimikujik National Park, Nova Scotia, J. Geophys. Res., 100, 2867–2881, 1995.

Song, X.-H., Polissar, A. V., and Hopke, P. K.: Sources of fine particle composition in the north-eastern US, Atmos. Environ., 35, 5277–5286, 2001.

Tereszchuk, K. A., González Abad, G., Clerbaux, C., Hadji-Lazaro, J., Hurtmans, D., Coheur, P.-F., and Bernath, P. F.: ACE-FTS observations of pyrogenic trace species in boreal biomass burning plumes during BORTAS, Atmos. Chem. Phys. Discuss., 12, 31629–31661, doi:10.5194/acpd-12-31629-2012, 2012.

USEPA: PM_{2.5} Mass Weighing Laboratory Standard Operating Procedures for the Performance Evaluation Program, Quality Assurance Guidance Document Method Compendium, 1–165, 1998.

Ward, T. J., Trost, B., Conner, J., Flanagan, J., and Jayanty, R. K. M.: PM_{2.5} source apportionment in a Subarctic airshed – Fairbanks, Alaska, Aerosol Air Qual. Res., 12, 536–543, doi:10.4209/aaqr.2011.11.0208, 2012.

Yin, J. and Harrison, R. M.: Pragmatic mass closure study for PM_{1.0}, PM_{2.5} and PM₁₀ at roadside, urban background and rural sites, Atmos. Environ., 42, 980–988, 2008.

Zhao, M., Zhang, Y., Ma, W., Fu, Q., Yang, X., Li, C., Zhou, B., Yu, Q., and Chen, L.: Characteristics and ship traffic source identification of air pollutants in China's largest port, *Atmos. Environ.*, 64, 277–286, doi:10.1016/j.atmosenv.2012.10.007, 2013.

ACPD

13, 4491–4533, 2013

Identifying sources driving observed PM_{2.5} variability

M. D. Gibson et al.

Title Page

Abstract

Introduction

Conclusions

References

Tables

Figures



Back

Close

Full Screen / Esc

Printer-friendly Version

Interactive Discussion



Identifying sources driving observed PM_{2.5} variability

M. D. Gibson et al.

Table 1. Descriptive statistics for the meteorological variables obtained at the DGS during the PM_{2.5} sampling period based upon 5-min average data.

	N	Mean	Std Dev	Min	25th Pctl	Median	75th Pctl	Max
Wind Speed (m s ⁻¹)	42	2.6	1.1	0.9	1.5	2.5	3.3	5.4
Temperature (°C)	42	19.6	6.3	15.5	17.4	19.2	20.1	58.4*
Relative Humidity (%)	42	84	9	64	78	84	91	97
Pressure (kPa)	42	100.2	0.4	99.1	99.9	100.2	100.6	101.1
Average Wind Vector: 238° ~ SW								

* considered an outlier (instrument malfunction)

[Title Page](#)
[Abstract](#)
[Introduction](#)
[Conclusions](#)
[References](#)
[Tables](#)
[Figures](#)
[Back](#)
[Close](#)
[Full Screen / Esc](#)
[Printer-friendly Version](#)
[Interactive Discussion](#)


Identifying sources driving observed PM_{2.5} variability

M. D. Gibson et al.

Title Page

Abstract

Introduction

Conclusions

References

Tables

Figures

◀

▶

◀

▶

Back

Close

Full Screen / Esc

Printer-friendly Version

Interactive Discussion



Table 2. Daily meteorological summary covering the filter sampling period 11 July 2011 to 25 August 2011 from Halifax International Airport.

11 Jul	Cloudy with mid day and afternoon sunshine. Wind S to SW 3 became SW 6–8 14:00. High 25.
12 Jul	Overnight fog then rain or showers to 18:00. Wind S 6–7 then light in eve. High 17.
13 Jul	Fog to 11:00 then mostly cloudy. Wind N at 6–8. High 23.
14 Jul	Clear to start then cloudy before sunrise with rain by 21.00. Wind N 6–8 and High 13
15 Jul	Rain ended at sunrise then cloudy then rain from 23:59. Wind N 6–11 . High 19.
16 Jul	Mostly cloudy with wind NW 8 then dropped off by 23:00. High 20.
17 Jul	Mostly clear to 12:00 then mostly cloudy. Wind SW 6. High 30
18 Jul	Mostly cloudy with a shower a noon. Clearing in evening. Wind SW 4–6. High 25.
19 Jul	Fog overnight then mostly cloudy with scattered shower at 16:00. Wind SW 3. High 26.
20 Jul	Mainly clear to 21:00 then cloudy. Wind W 3 except SW 8 at 21:00 then SW 6–7. High 27.
21 Jul	Cloudy then Rain Fog and a Thundershower in late evening. Wind SW 6–8 except 12 late evening. High 28.
22 Jul	Fog to 14:00 then mostly cloudy. Wind W 3 then light then SE 6 then N 4. High 28.
23 Jul	Fog to 14:00 then mostly cloudy, 20:00 shower then Fog. Wind light N then S 4–6
24 Jul	Clear early morning then mostly cloudy then clear in evening. Wind NW-N 4–6 then light in the evening. High 23.
25 Jul	Clear. Wind light. Then S 4 from mid afternoon. High 24.
26 Jul	Clear at first then mostly cloudy to cloudy with fog in the evening. Wind SE 4–6 light in the eve.
27 Jul	Fog to mid day then cloud with supertime showers. Wind SE 3. High 19.
28 Jul	Fog early then mostly cloudy. Wind NW-N 4. High 20.
29 Jul	Clear then mostly cloudy after 09:00. Wind light then SW 6–7 after midday. High 23.
30 Jul	Fog to morning then mostly rain through day – drizzle in the evening. Wind S-SE 4–6 became N 7 late eve. High 18.
31 Jul	Mostly cloudy except clear midday and then in evening. Wind NW 4–6. High 25.

Data Meteorological Data Summary Key: Dates in **bold italics** indicate a date with significant sunshine (≥ 6 h). Dates in **bold** indicate a date with precipitation > 0.2 mm. **Descriptive text in bold** highlights a significant meteorological feature. Wind speed (ms^{-1}). Temperature ($^{\circ}\text{C}$). Time in UTC.

Table 2. Continued.

1 Aug	Clear to sunrise then mostly cloudy to sundown. Wind light then SE 4 after noontime. High 24.
2 Aug	Fog then cloudy. Thunderstorms from mid afternoon through evening. Wind SE 6–8. High 22.
3 Aug	Thunderstorms and rain until 07:00 then cloudy, showers in the morning. Wind ESE 6–8. High 17.
4 Aug	Cloudy, showers to midday. Wind NE 4–6. High 18.
5 Aug	Mostly cloudy to late evening. Wind N 4–7. High 19.
6 Aug	Fog overnight then mainly clear after 12:00. Wind NW 3 then light in evening. High 24.
7 Aug	Cloudy to late morning then some sun. Rain late evening. Wind S-SE 3. High 25.
8 Aug	Fog, Drizzle and showers then rain by midday ended in the evening. Wind S-SE 4–6. High 19.
9 Aug	Fog overnight then cloudy with evening drizzle. Wind N 6–8 then light in evening. High 20.
10 Aug	Fog and Drizzle to midmorning then cloudy. Showers in the evening. Wind SE 6 occasionally 8 . High 16
11 Aug	Fog then morning drizzle then cloudy with some late day sun. Wind SE 4–6. High 19.
12 Aug	Some early morning fog otherwise clear. Wind W 1–3 then SE 4 later afternoon. High 24.
13 Aug	Clear. Light except NW 4 midday hours. High 25.
14 Aug	Clear then mostly cloudy in the afternoon. Wind SW 4–6. High 26.
15 Aug	Fog then mostly cloudy with eve showers and rain. Wind SE 3–4. High 23.
16 Aug	Rain and drizzle. Clear to supper. Then Cloudy with late drizzle. Wind SE 6 then to 8 in the afternoon.
17 Aug	Showers and drizzle end overnight. Then clear by 13:00. Wind NW 6. High 24.
18 Aug	Clear. Wind light SW then S-SW 6–8. High 25.
19 Aug	Fog patches to sunrise then cloudy but Clear by noon. Wind SW 3–4 then S 6 from mid afternoon. High 25.
20 Aug	Fog patches overnight then mostly cloudy with sunny periods. Clear late eve. Wind SW-S 4–7. High 26.
21 Aug	Fog overnight. Then clear in the am then mostly cloudy. Wind S-SW 10 becoming 6–7 at 16:00.
22 Aug	Cloudy with overnight fog. Rain showers from mid afternoon onward. Wind S 6–8 with G 11. High 22.
23 Aug	Mainly clear. Wind NW 4–6 becoming W 3–4 late in the day. High 23.
24 Aug	Clear then mostly cloudy from 15:00 onwards. Wind W 3 but SSW 6–8 in afternoon and evening. High 24.
25 Aug	Few sunrise fog patches. Otherwise Clear to early afternoon then cloudy. Wind S 3–4 then SSW 8–11 dropping to SSW 6 in evening. High 25. Remnants of TS. Irene forecast for Sunday the 28th.
Precipitation Summary: 17 days with more than 0.2 mm. Heavy precipitation days > 20mm: 20 Jul, 2 Aug and 8 Aug.	

Identifying sources driving observed PM_{2.5} variability

M. D. Gibson et al.

Title Page

Abstract Introduction

Conclusions References

Tables Figures

◀ ▶

◀ ▶

Back Close

Full Screen / Esc

Printer-friendly Version

Interactive Discussion



Identifying sources driving observed PM_{2.5} variability

M. D. Gibson et al.

Title Page

Abstract

Introduction

Conclusions

References

Tables

Figures

◀

▶

◀

▶

Back

Close

Full Screen / Esc

Printer-friendly Version

Interactive Discussion



Table 3. Descriptive statistics of PM_{2.5} mass ($\mu\text{g m}^{-3}$) and species mass ($\mu\text{g m}^{-3}$) used in the PMF analysis.

	<i>n</i>	Mean	Std	Min	25th Pctl	Median	75th Pctl	Max	Data Completeness %	LOD
Total PM _{2.5}	45	4.5	3.4	0.08	2.1	3.9	5.6	13.7	100	0.04
Black Carbon	45	0.41	0.21	0.12	0.26	0.39	0.52	1.03	100	0.01
Organic Matter	45	1.05	0.72	0.18	0.48	0.77	1.50	2.77	85	0.10
Al	45	0.020	0.016	0.0091	0.0091	0.011	0.028	0.086	100	0.0070
As	45	0.0010	0.00076	0.00015	0.00054	0.00087	0.00114	0.0040	100	0.00010
Ba	45	0.0063	0.0020	0.0031	0.0056	0.0056	0.0063	0.0163	100	0.0026
Br	45	0.0015	0.00079	0.00095	0.0010	0.0013	0.0017	0.0047	100	0.00086
Ca	45	0.017	0.019	0.0021	0.0089	0.014	0.016	0.13	100	0.0015
Cl	45	0.046	0.070	0.0019	0.0042	0.011	0.045	0.32	100	0.0015
Cr	45	0.0022	0.00079	0.00035	0.0017	0.0020	0.0027	0.0040	100	0.00030
Cu	45	0.0013	0.00050	0.00062	0.00095	0.0013	0.0015	0.0028	100	0.00060
Fe	45	0.0240	0.0200	0.00110	0.0110	0.0180	0.0280	0.0970	100	0.00065
K	45	0.023	0.019	0.0017	0.011	0.018	0.027	0.11	100	0.0010
Mg	45	0.017	0.018	0.0039	0.0060	0.014	0.020	0.11	100	0.0035
Mn	45	0.00031	0.00029	0.00010	0.00010	0.00025	0.00036	0.0017	100	0.00005
Na	45	0.11	0.12	0.0089	0.037	0.090	0.13	0.73	100	0.00081
NH ₄	45	0.23	0.27	0.0030	0.066	0.15	0.27	1.45	100	0.0010
Ni	45	0.0011	0.00078	0.00044	0.00046	0.00070	0.0015	0.0037	100	0.00016
NO ₃	45	0.093	0.10	0.0074	0.042	0.067	0.10	0.64	100	0.0030
P	45	0.0020	0.0017	0.000040	0.00079	0.0015	0.0023	0.0081	100	0.000010
Pb	45	0.00037	0.00035	0.000060	0.00014	0.00027	0.00050	0.0017	100	0.000032
S	45	0.39	0.34	0.0022	0.18	0.29	0.42	1.81	100	0.0009
Se	45	0.00019	0.00027	0.000080	0.000080	0.000080	0.000080	0.0015	100	0.00008
Si	45	0.042	0.048	0.0044	0.014	0.030	0.056	0.29	100	0.0036
SO ₄	45	0.78	0.97	0.14	0.26	0.47	0.70	5.59	100	0.070
Sr	45	0.00055	0.00034	0.000010	0.00041	0.00049	0.00060	0.0021	100	0.000010
V	45	0.0033	0.0027	0.0016	0.0016	0.0026	0.0038	0.017	100	0.00092
Zn	45	0.0023	0.0017	0.00070	0.0012	0.0019	0.0030	0.0089	100	0.00051

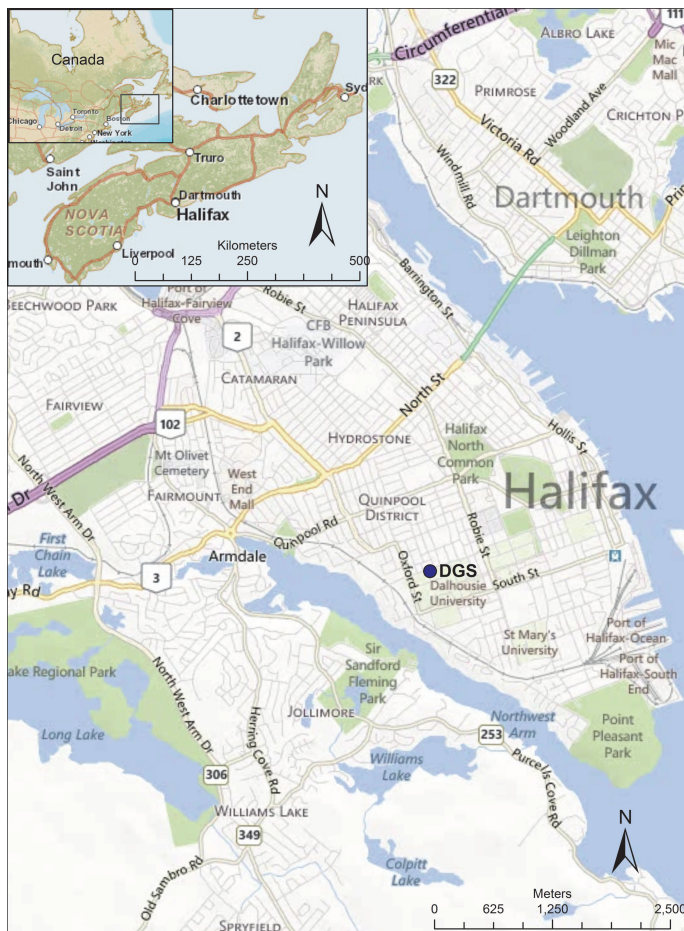


Fig. 1. Location of the DGS used during BORTAS-B (source of maps: free within ArcGIS v10).

Identifying sources driving observed PM_{2.5} variability

M. D. Gibson et al.

Title Page	
Abstract	Introduction
Conclusions	References
Tables	Figures
◀	▶
◀	▶
Back	Close
Full Screen / Esc	
Printer-friendly Version	
Interactive Discussion	



Identifying sources driving observed PM_{2.5} variability

M. D. Gibson et al.

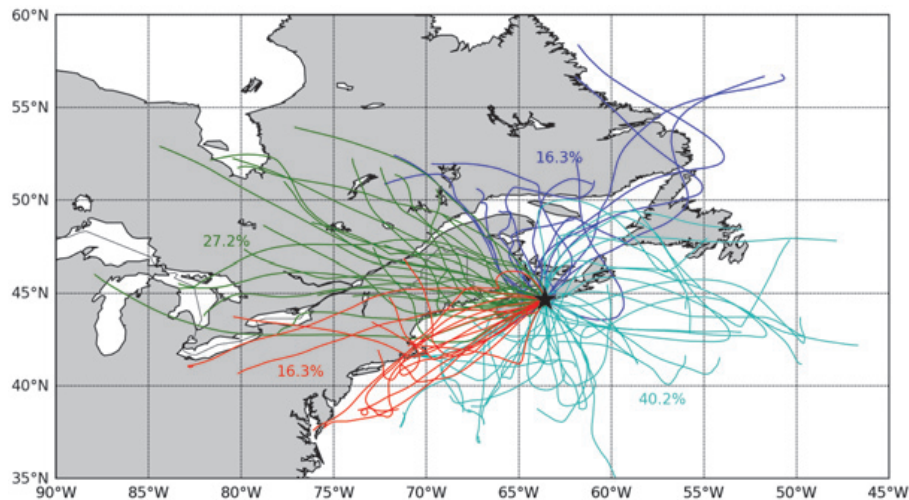


Fig. 2. Map of ensemble HYSPLIT 2-day air mass back trajectories between 11 July 2011 and 25 August 2011. Trajectories were initialized 08:00 UTC with an arrival height of 500 m. Colours denote upwind source region (cyan = Marine, red = SW, green = WNW and blue = N).

[Title Page](#)[Abstract](#)[Introduction](#)[Conclusions](#)[References](#)[Tables](#)[Figures](#)[◀](#)[▶](#)[◀](#)[▶](#)[Back](#)[Close](#)[Full Screen / Esc](#)[Printer-friendly Version](#)[Interactive Discussion](#)

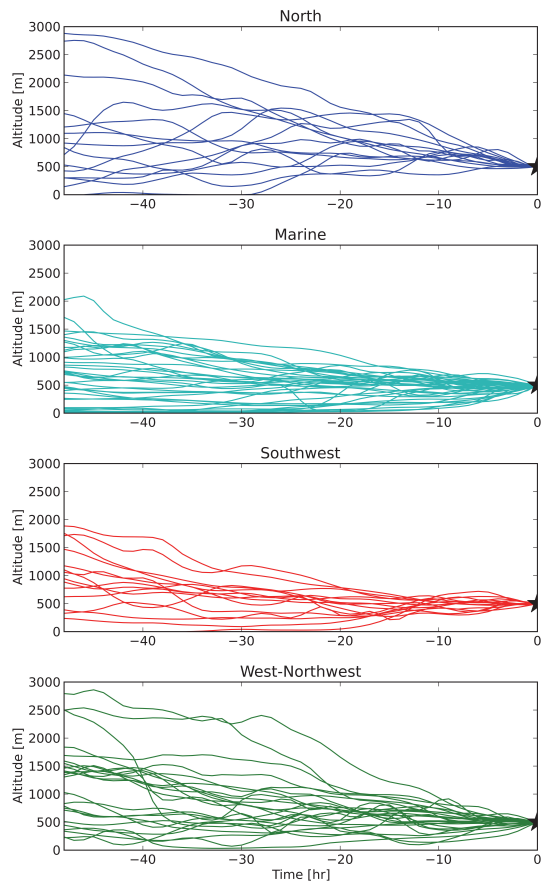


Fig. 3. HYSPLIT 2-day air mass back trajectory vertical profiles.

Identifying sources driving observed PM_{2.5} variability

M. D. Gibson et al.

Title Page

Abstract

Introduction

Conclusions

References

Tables

Figures

◀

▶

◀

▶

Back

Close

Full Screen / Esc

Printer-friendly Version

Interactive Discussion



Identifying sources driving observed PM_{2.5} variability

M. D. Gibson et al.

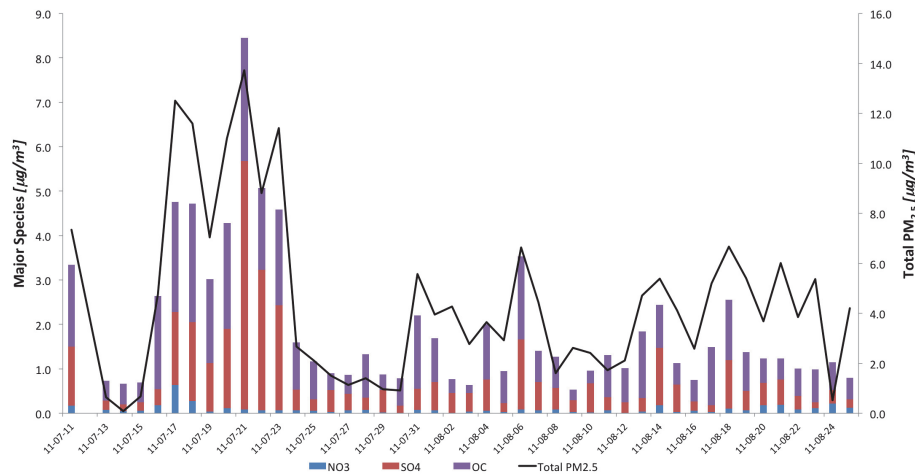


Fig. 4. Time series of total PM_{2.5} mass and major species concentration.

Title Page

Abstract

Introduction

Conclusions

References

Tables

Figures

⏪

⏩

◀

▶

Back

Close

Full Screen / Esc

Printer-friendly Version

Interactive Discussion



Identifying sources driving observed PM_{2.5} variability

M. D. Gibson et al.

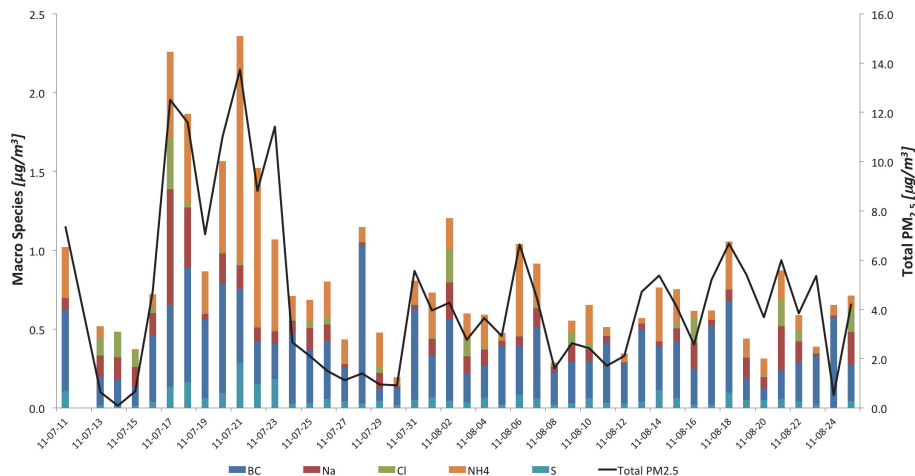


Fig. 5. Time series of total PM_{2.5} mass and macro species concentration.

Title Page

Abstract

Introduction

Conclusions

References

Tables

Figures

⏪

⏩

◀

▶

Back

Close

Full Screen / Esc

Printer-friendly Version

Interactive Discussion



Identifying sources driving observed PM_{2.5} variability

M. D. Gibson et al.

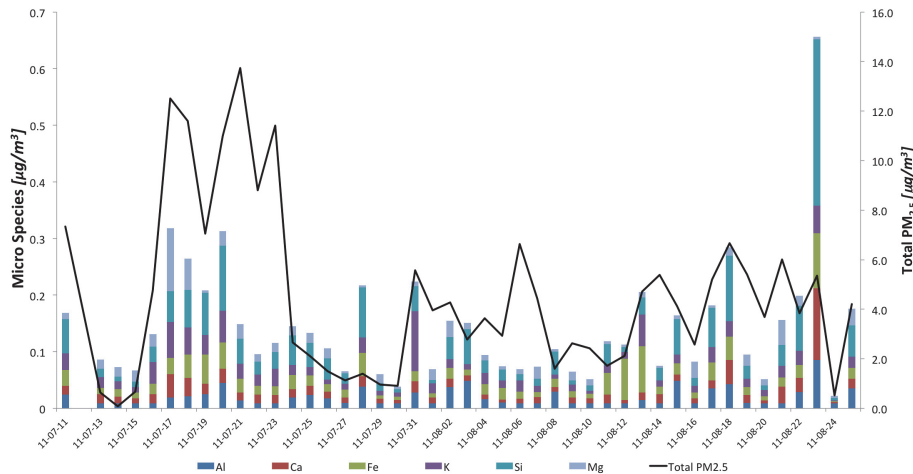


Fig. 6. Time series of total PM_{2.5} mass and micro species concentration.

Title Page

Abstract

Introduction

Conclusions

References

Tables

Figures

◀

▶

◀

▶

Back

Close

Full Screen / Esc

Printer-friendly Version

Interactive Discussion



Identifying sources driving observed PM_{2.5} variability

M. D. Gibson et al.

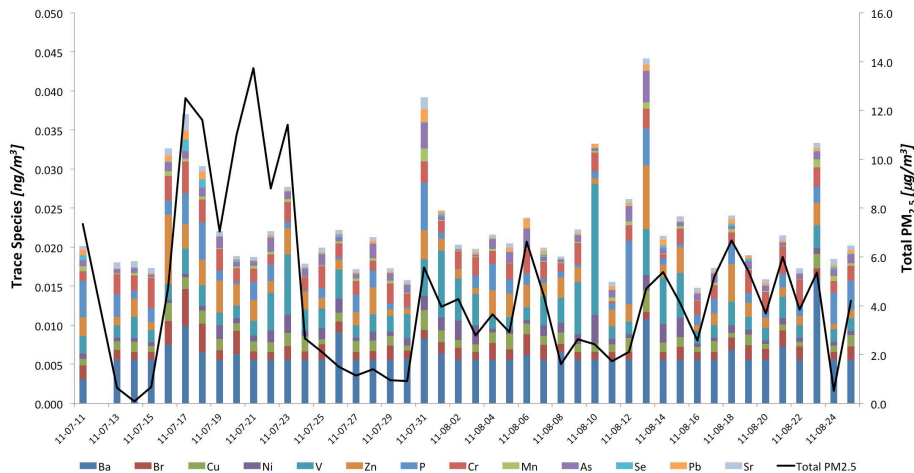


Fig. 7. Time series of total PM_{2.5} mass and trace species concentration.

Title Page

Abstract

Introduction

Conclusions

References

Tables

Figures

⏪

⏩

◀

▶

Back

Close

Full Screen / Esc

Printer-friendly Version

Interactive Discussion



Identifying sources driving observed PM_{2.5} variability

M. D. Gibson et al.

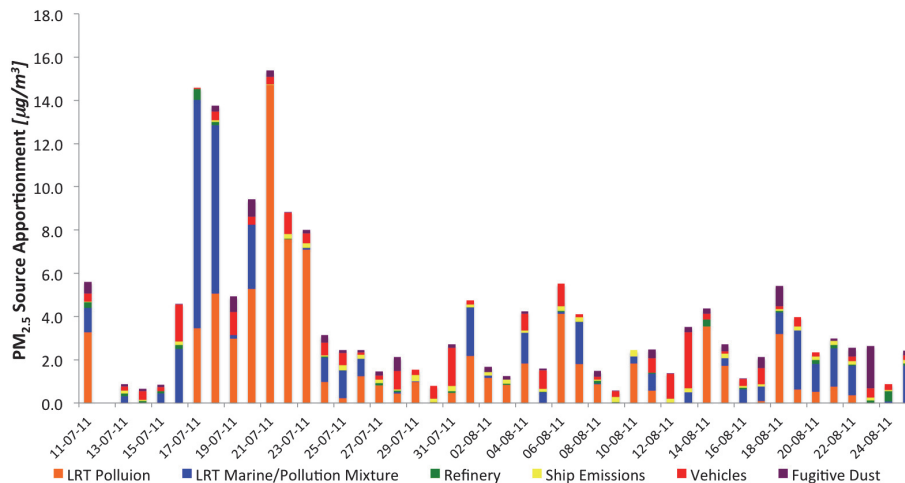


Fig. 8. Time series of PM_{2.5} source apportionment based upon PMF output.

Title Page

Abstract

Introduction

Conclusions

References

Tables

Figures

◀

▶

◀

▶

Back

Close

Full Screen / Esc

Printer-friendly Version

Interactive Discussion



Identifying sources driving observed PM_{2.5} variability

M. D. Gibson et al.

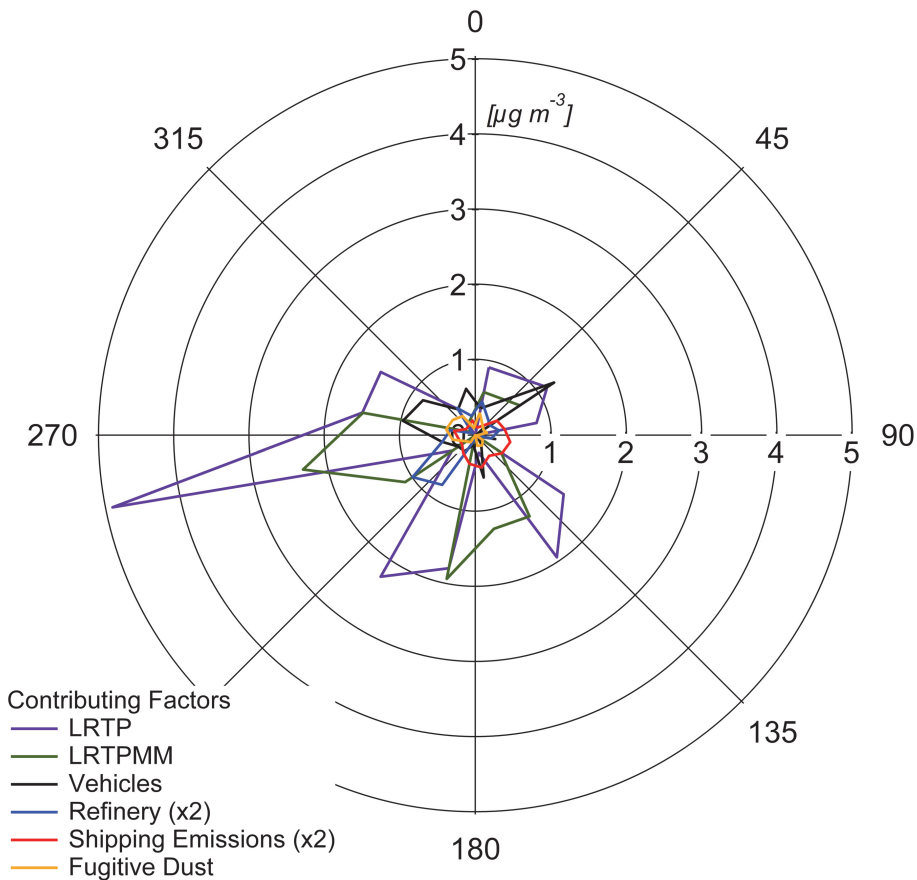


Fig. 9. Source Contribution Rose.

Title Page

Abstract

Introduction

Conclusions

References

Tables

Figures

◀

▶

◀

▶

Back

Close

Full Screen / Esc

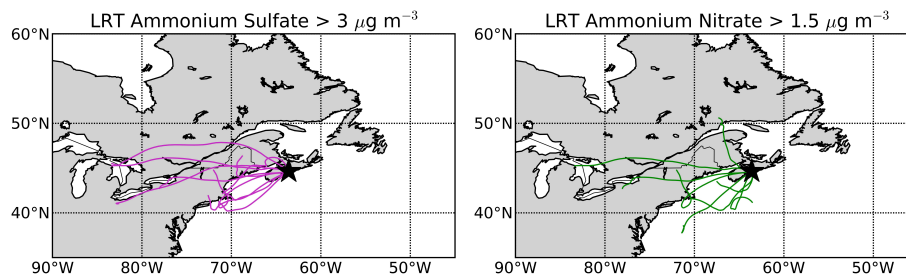
Printer-friendly Version

Interactive Discussion



Identifying sources driving observed PM_{2.5} variability

M. D. Gibson et al.

**Fig. 10.** Back trajectories associated with the highest values of each PMF cluster.

Title Page

Abstract

Introduction

Conclusions

References

Tables

Figures

◀

▶

◀

▶

Back

Close

Full Screen / Esc

Printer-friendly Version

Interactive Discussion



Identifying sources driving observed PM_{2.5} variability

M. D. Gibson et al.

Title Page

Abstract

Introduction

Conclusions

References

Tables

Figures

◀

▶

◀

▶

Back

Close

Full Screen / Esc

Printer-friendly Version

Interactive Discussion

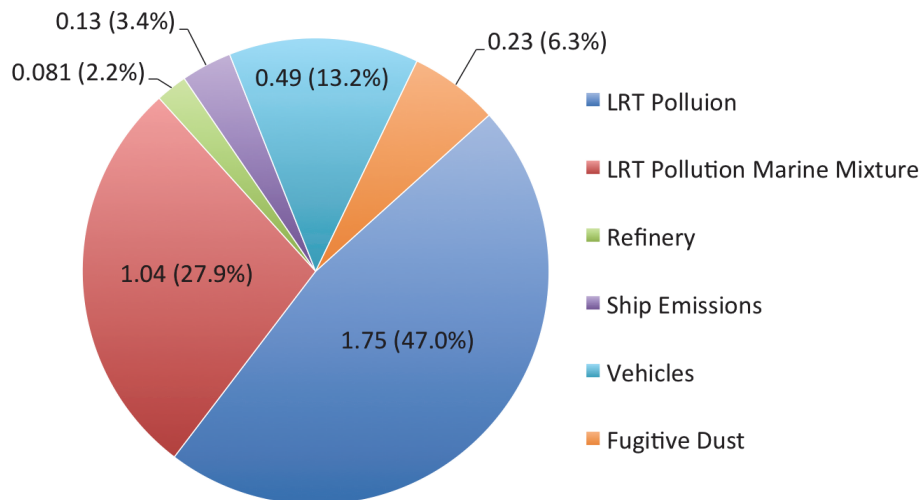


Fig. 11. Average mass concentration ($\mu\text{g m}^{-3}$) of attributed sources and percentage source contributions over the 45 days of sampling.